PHYSICAL REVIEW D **93,** 083010 (2016)

Mitigating parametric instability in optical gravitational wave detectors

Andrey B. Matsko,[1] Mikhail V. Poplavskiy,[2] Hiroaki Yamamoto,[3] and Sergey P. Vyatchanin[2]
[1]*OEwaves Inc., 465 North Halstead Street, Suite 140, Pasadena, California 91107, USA*
[2]*Faculty of Physics, Lomonosov Moscow State University, Moscow 119991, Russia*
[3]*LIGO Laboratory, California Institute of Technology, MC 100-36, Pasadena, California 91125, USA*
(Received 11 January 2016; published 19 April 2016)

Achieving quantum limited sensitivity in a laser interferometric gravitational wave detector can be hindered by an optomechanical parametric instability of the interferometer. This instability is sustained by a large number of idle high-finesse Stokes modes supported by the system. We show that by optimizing the geometrical shape of the mirrors of the detector, one reduces the diffraction-limited finesse of unessential optical modes and effectively increases the instability threshold. Utilizing parameters of the Advanced LIGO system as a reference, we find that the proposed technique allows constructing a Fabry-Perot interferometer with round-trip diffraction loss of the fundamental mode not exceeding 5 ppm, whereas the loss of the first dipole as well as the other high-order modes exceeds 1000 ppm and 8000 ppm, respectively. This is 2 orders of magnitude higher if compared with a conventional Advanced LIGO interferometer. The optimization comes at the price of tighter tolerances on the mirror tilt stability, but it does not result in a significant modification of the optical beam profile and does not require changes in the gravity detector readout system. The cavity with proposed mirrors is also stable with respect to the slight modification of the mirror shape.

DOI: 10.1103/PhysRevD.93.083010

I. INTRODUCTION

Gravitational wave astronomy inherently relies on high-power resonant optical systems. The power of the probe light circulating in a cavity is the ultimate lever utilized to increase the sensitivity of a position measurement of gravitational wave detector test masses carrying information about gravitational wave signals. The projected power, circulating in the arms, pushes a 0.8 MW value in the second generation of gravitational wave detectors such as Advanced LIGO (now in operation), Advanced VIRGO, and KAGRA [1–5]. While this power value is by far lower if compared with the optical damage limit of the cavity mirrors, it is high enough to initiate various nonlinear processes, including parametric instability [6], thermal lensing [7], and alignment (tilt) instability [8], resulting in depletion of the probe light and generation of optical harmonics, adding noise to the recorded signal and hindering the desirable sensitivity increase. Technical solutions allowing suppression of the nonlinear interactions are needed to push the limits of gravitational wave astronomy and to widen the horizon of observable events associated with gravitational wave emission.

Resonant optomechanical oscillations caused by undesirable parametric instability (PI) [6,9–15] are expected to have the lowest power threshold if compared with the other nonlinear processes in the cavities. The PI occurs due to interaction of optical cavity modes and mechanical modes of the cavity mirrors. The photons of the probe light confined in a selected, usually fundamental, cavity mode pumped at frequency ω_p are parametrically converted to mechanical phonons of the cavity mirrors (having frequency Ω_m) as well as lower-frequency, or Stokes, photons emitted into high-order optical modes having frequency $\omega_s \simeq \omega_p - \Omega_m$. The power threshold of the PI is inversely proportional to the product of quality factors of the optical and mechanical modes participating in the process, in other words, desirable reduction of the optical as well as mechanical attenuation results in undesirable reduction of the PI threshold. A method of PI reduction not associated with decrease of the quality of the modes is needed.

The phenomenon of PI was studied and validated experimentally in a tabletop Fabry-Perot resonator [16] as well as in whispering gallery mode resonators [17–19]. Recently PI was observed in the full-scaled Advanced LIGO interferometer [20] at relatively small circulating power ~50 kW as compared with 800 kW planned in Advanced LIGO. The first observation of gravitational waves was achieved with 100 kW power [5].

Efficiency of PI depends on phase matching, comprising nonzero overlap integral and energy conservation, of the optical and mechanical modes. There is a significant probability that these conditions are always fulfilled in long-base gravitational wave detectors because of the dense spectrum of optical modes of large cavities and the dense spectrum of mechanical modes of large-area cavity mirrors. Since the mirrors involved in the system are not identical, they have slightly different associated mechanical frequencies that increase PI probability.

Several techniques reducing PI impact have been studied recently. They involve either breaking the phase matching of the nonlinear process by changing the frequency spectra

of the modes participating in the PI process, or reducing PI efficiency by damping nonessential modes.

For instance, one can move the optomechanical system out of resonance by controlling and modulating the surface temperature of the mirrors [21–24]. This is possible since the optical (ω_p and ω_s) and mechanical (Ω_m) eigenfrequencies of the system depend on the mirror temperature T in different ways, so the PI favorable condition $\omega_p(T) = \omega_s(T) + \Omega_m(T)$ ultimately breaks. The drawback of this technique is related to its lack of selectivity. All the modes of the optical cavity move at nearly the same pace, and while one pair of Stokes and mechanical modes comes out of the resonance, another pair comes in. This drawback can be partially suppressed by modulation of the temperature of the mirror surface.

An alternative stabilization method involves damping mechanical modes in either a passive or an active way. It was proposed that an acoustic mode damper [25] as well as introducing an annular strip at the rims of cavity mirrors reduces the quality (Q) factors of elastic modes [22,26,27]. However, this strip reduces the Q factor of the modes within the whole spectrum, including reception band of the antenna (30…500 Hz). This is undesirable, since low mechanical attenuation at these frequencies is essential for achieving the desirable detection sensitivity.

Active electromechanical feedback allows reducing the Q factor of several particular elastic modes [28,29]. The method is too selective to suppress all the high-frequency modes in the entire frequency band of interest (50…200 kHz), and hence does not solve the problem of instability of highly overmoded optomechanical systems. Therefore, a universal method of PI suppression is still needed.

We propose here a universal solution based on optimization of the shape of the cavity mirrors leading to increase of the diffraction losses of all high-order optical modes of the realistic optical cavity and subsequent increase of the PI threshold. It is known that the diffraction loss of selected modes of a cavity having large-area mirrors can be increased rather significantly by properly shaping the mirrors [30–32]. The Q factor of the lowest-order (fundamental or main) modes of the cavity does not suffer in this case. However, this analysis does not work in the case of realistic finite mirrors, since this kind of mirror shaping is associated with unacceptable loss increase of the fundamental family of the cavity.

We have found that the loss increase can be circumvented and have developed a technique that allows realizing an optical cavity containing only one family of low-loss fundamental bounded modes for the case of the finite mirror size. We have demonstrated the feasibility of the method using an example of a Fabry-Perot interferometer with parameters close to the Advanced LIGO interferometer and have shown that the idea is feasible for the increase of the PI threshold at least by an order of magnitude, keeping diffraction loss of the main mode family at an acceptable low level. Since the shaping of the mirrors results in enhancement of the dependence of the round-trip diffraction loss on the mirror tilt, we have developed a semianalytical theory of this phenomenon and have shown that such dependence becomes acceptable for the case of carefully optimized mirror shape. Finally, we have found that the optimized cavity can still be interrogated using conventional Gaussian beams. We discuss the results in what follows.

II. THRESHOLD CONDITION

The lowest intracavity threshold power of the PI evaluated for a Fabry-Perot (FP) resonator can be found from the expression [6]

$$P_{\rm th} = \frac{Mc^2\Omega_m^2\mathcal{L}}{4\zeta\omega_s Q_m},$$
$$\zeta = \frac{V|\int f_p(\vec{r}\perp) f_s(\vec{r}_\perp)\vec{u}_z(\vec{r})d\vec{r}_\perp|^2}{\int|\vec{f}_p(\vec{r}_\perp)|^2 d\vec{r}_\perp \int|\vec{f}_s(\vec{r}_\perp)|^2 d\vec{r}_\perp \int|\vec{u}(\vec{r})|^2 dV}, \qquad (1)$$

where $\mathcal{L}$ is the round-trip optical power attenuation coefficient of the Stokes mode, M is the mass of the mirror, or test mass, Q_m is the quality factor of the elastic mode, c is the speed of light in the vacuum, ζ is a mismatching factor, V is the volume of the mirror, $\vec{u}(\vec{r})$ is the mechanical mode displacement, u_z is the same normal displacement on the mirror surface, and f_p, f_s are the field amplitude mirror surface distributions for the main and Stokes optical modes. The integration is performed over the volume (dV) and surface ($d\vec{r}_\perp$) of the mirror.

Equation (1) is obtained for the all-resonant case: $\omega_p = \omega_s + \Omega_m$. Substituting into Eq. (1) the parameters of the Advanced LIGO system, presented in Table I, and assuming complete overlap of the modes ($\zeta = 1$), we find that the PI threshold power, $P_{\rm th}$, is more than 2 orders of magnitude smaller if compared with the envisioned power level P [6]. To increase the threshold towards the desirable value, we propose to increase $\mathcal{L}$ to 8000 ppm (it corresponds to $P_{\rm th} = 1$ MW at $M = 40$ kg, $\Omega_m = 5 \times 10^5$ sec^{-1}, $Q_m = 10^6$, $\zeta = 1$, and parameters in Table I) by inducing leakage of the Stokes light out of the cavity due to enhanced diffraction of the high-order optical modes. This increase results in a small practically acceptable increase of the attenuation of the fundamental mode $\mathcal{L}_p = 5$ ppm. The loss limits the degree of improvement of the sensitivity of the measurements if quantum squeezed light is used in the system, and $\mathcal{L}_p = 5$ ppm is acceptable for the realistically projected values of the achievable degree of squeezing. It is also worth noting that in reality the overlap is not complete ($\zeta < 1$), and the requirement to the reduction of the finesse for the high-order modes is less stringent.

The idea of the method relies on a dependence of the attenuation of high-order modes of a FP cavity on relatively small deviations of the cavity mirror shape from the spherical

TABLE I. Parameters of Advanced LIGO used in calculations (radii of curvature are different for the input and output mirrors in the arms of the real Advanced LIGO interferometer; we use the mean value for both).

Parameter	Value
Arm length, L	4 km
Optical wavelength, λ	1064 nm
Intracavity power, P	800 kW
AS_{00} (main Gaussian) mode round-trip loss, $\mathcal{L}_p$	0.45 ppm
D_{10} (LG_{10}) dipole mode round-trip loss, $\mathcal{L}$	10 ppm
Characteristic cavity length $b=\sqrt{L\lambda/2\pi}$	0.0260 m
Radius of mirrors, r_m	0.17 m
Dimensionless mirror radius $a_m=R/b$	6.53
Radius w of laser spot at the mirror for TEM00 mode	0.06 m
Radius w_0 of laser beam at the waist	0.0115 m
Curvature radius of spherical mirrors, R_c	2076 m
Geometric parameter $g=1-L/R_c$ of the cavity	−0.92649
Gouy phase, $\arctan[(b/w_0)^2]$	1.378

one. The diffraction loss of the fundamental axially symmetric mode decreases exponentially with the mirror diameter in a properly designed cavity, while the loss of the other modes follows a power-law dependence on the diameter. The ratio of round-trip loss of the fundamental and the higher-order optical modes of a cavity should exceed 2 orders of magnitude to be acceptable for the application. To compare, the current Advanced LIGO cavity has this ratio fixed at the level of 20 for the main and the first dipole modes (see Table I). As shown in the next section, minute modifications of the Advanced LIGO mirror shape, keeping the overall mirror size intact, results in a significant increase of the round-trip loss of unwanted optical modes and an increase of the PI threshold towards desirable numbers.

III. MIRROR SHAPE OPTIMIZATION

We consider resonators having a nearly Gaussian spatial profile of the lowest-order modes to ensure that the conventional auxiliary optics can be utilized with them. This is essential for the postprocessing of the output light, requiring perfect matching with the modes of conventional filtering cavities, as well as local oscillators involved in the data acquisition. This condition should be fulfilled if the curvature of the mirrors stays the same as the curvature of spherical mirrors of the conventional cavity at the symmetry axis of the cavity. The curvature deviates from the conventional one away from the symmetry axis. Finding the optimal shape of the cylindrically symmetric mirrors is the major task we solve here.

We introduce dimensionless variables and parameters:

$$x=\frac{r}{b},\qquad b=\sqrt{\frac{L\lambda}{2\pi}},\qquad \rho=\frac{R_c}{L},\qquad a_m=\frac{r_m}{b},\tag{2}$$

where r is the distance from the center of the mirror, b is a scaling factor, L is the distance between mirrors, λ is a wavelength, R_c is the curvature radius of the mirror, and r_m is the radius of the mirror. The shape of the mirrors of the FP cavity is described by

$$y=y_0(1-e^{-z-\alpha z^2-\beta z^3}),\qquad z=\frac{x^2}{2\rho y_0},\tag{3}$$

where α, β, and y_0 are dimensionless independent parameters we optimize. The profile (3) transforms into a spherical one $y=x^2/2\rho$ at $y_0\to\infty$ (or at $x\to 0$). There are many ways of defining the mirror profile. We selected this particular one because it allows adjusting the radius of the mirror curvature in a very broad range.

While a fundamental understanding of the optimization procedure can be gained from the Born-Oppenheimer approach applied to a FP cavity, an accurate analytical optimization of the mirror shape is unfeasible, so numerical simulations have to be used. We utilize a matrix analogue of the Fresnel integral to find electric field distribution $\Psi^{\rm right}$ at the right mirror surface of the FP resonator using the distribution $\Psi^{\rm left}$ at the left mirror (and vice versa): $\Psi^{\rm right}=RPR\Psi^{\rm left}$, where the matrix P describes the propagation from the left plane to the right one and depends on the mode of the cavity; the diagonal matrix R describes the shapes of the mirrors. The equation $(RPR)^2\Psi=\Lambda\Psi$ is solved numerically, and round-trip loss is found from $\mathcal{L}=1-|\Lambda|^2$.

Following the approach described in Refs. [33,34], we define the propagation matrix for axial symmetric (AS) modes through Hankel transform as

$$P=H^+G(H^+)^{-1},\qquad G_{kn}=\exp\left(-i\frac{\xi_k^2}{2a^2}\right)\delta_{nk},\tag{4}$$

$$H^+_{kn}=\frac{4\pi a^2}{\xi_N^2N_n}J_0\left(\frac{\xi_k\xi_n}{\xi_N}\right),\qquad N_n=\left[1+\frac{1}{\xi_n^2}\right]J_0(\xi_n^2),\tag{5}$$

where $a=Sa_m$, $S>1$ is the simulation window parameter, which may vary between 1.5 and 5; J_0 and J_1 are Bessel functions of the first kind; and ξ_n is the set of the first N roots of the characteristic equation $J_0(\xi)-\xi J_1(\xi)=0$.

The propagator P for the azimuthal higher-order modes (the field depends on the azimuthal angle ϕ as $\sim e^{in\phi}$, where n is an integer) is easy to generalize. For example, for dipole modes with dependence $\sim e^{i\phi}$ we have to substitute J_1 instead of J_0 into (5) and to use roots of the characteristic equation $J_1(\xi)-\xi J_2(\xi)=0$.

The mirror shape is presented numerically by the matrix

$$R_{kn}=d_ke^{-iy(x_n)}\delta_{kn},\qquad x_n=\xi_na/\xi_N,\tag{6}$$

$$d_k=\begin{cases}1, & \text{if } x_n<a_m,\\ 0, & \text{if } x_n>a_m,\end{cases}\tag{7}$$

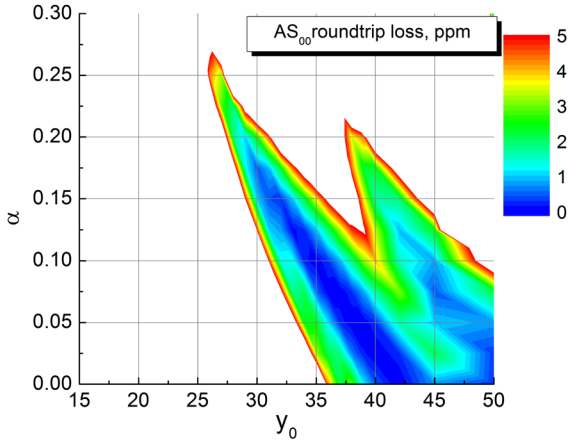

FIG. 1. Dependence of AS_{00} mode round-trip loss (ppm) on mirror shape parameters in the range $y_0 = 15$–50 and $\alpha = 0$–0.3.

where the coefficients d_k define reflective surface of the mirror.

Selecting the number of points $N = 512$ and the parameter of the window $S = 2$, we have found the dependence of the attenuation parameters of various modes of the cavity on the mirror shape (Fig. 1). As the rule, the first dipole mode (D_{10}) has the lowest loss with respect to the fundamental axially symmetric mode (AS_{00}). We optimized the problem by identifying local maxima of the ratio of attenuation of the dipole and the fundamental mode, as illustrated by Figs. 2 and 3. Several identified local optima for the mirror shape are listed in Table II. We have selected the radius of curvature in the center of the deformed mirrors to be $R_c = 2014$ m; it corresponds to a spot radius $w = 0.09$ m for the spherical mirror. However, due to change of the mirror shape, as described below, the spot size decreased to $w \simeq 0.05$ cm, even though the radius of curvature of the mirrors did not change in the vicinity of the symmetry axis. The simulation shows that modification of the mirror shape results in significant increase of

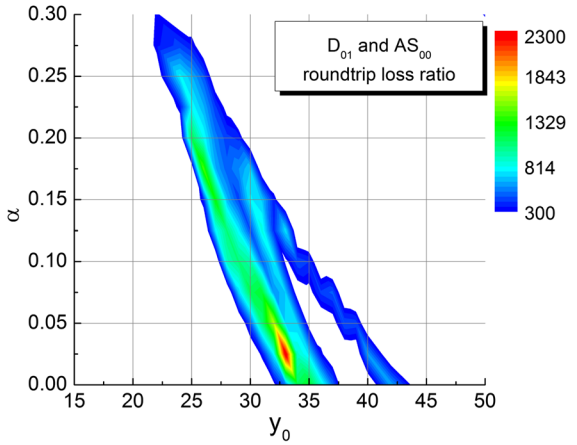

FIG. 2. Dependence of the attenuation ratio D_{10} to AS_{00} on mirror shape parameters in the range $y_0 = 15$–50 and $\alpha = 0$–0.3.

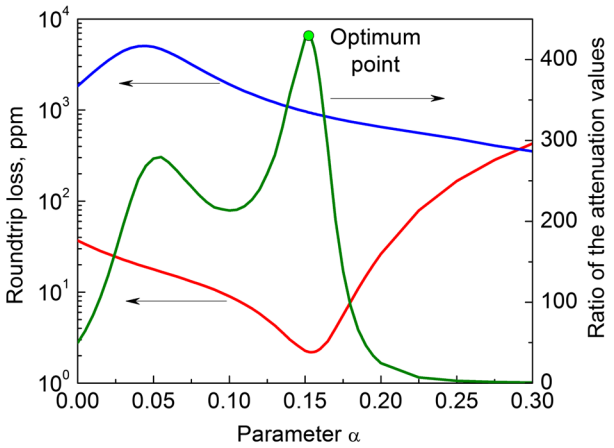

FIG. 3. Searching for the local optimum point under the following conditions: AS_{00} round-trip loss (red curve) does not exceed 5 ppm, D_{10} round-trip loss (blue curve) is approximately 10^3 ppm, and the ratio of these losses (green curve) reaches a local maximum. This figure corresponds to parameter set 1 in Table II.

diffraction loss of the high-order modes while keeping the attenuation of the fundamental modes low. One can see from Table II that practically all the higher-order modes demonstrate loss larger than ~8000 ppm level defined in Sec. II, with the exception only of the dipole modes having approximately 1000 ppm loss (all the modes that are not listed in Table II have higher diffraction loss, exceeding 8000 ppm).

It is important to confirm that the cavity with the deformed mirrors can be interrogated using conventional Gaussian beams. We have found that the amplitude distribution of the modes of interest only slightly differs from the Gaussian fit having the same full width at the half maximum (corresponding to a spot radius of about 0.05 m), as shown in Fig. 4, in spite of the significant difference of mirror shapes shown in Fig. 5. Normalizing the electric field amplitude of the modes over the beam cross section according to $\int |E|^2 dS = 1$, we have found that the mismatch between the matching Gaussian beam and the cavity eigenmode is small for any of the selected mirror shapes. The mismatch is determined as $\int (|E_{AS00}| - E_{\mathrm{Gauss}})^2 dS < 10^{-3}$. In particular, for parameter set 3 in Table II, we calculated the overlap integral in the form $\int (|E_{AS00}| E_{\mathrm{Gauss}})^2 dS \simeq 0.9995$, whereas taking into account the imaginary part, $|\int (E_{AS00} E_{\mathrm{Gauss}})^2 dS| \simeq 0.9768$, which also confirms that the cavity with the optimized mirrors can be pumped using Gaussian beams, and the quantum state of the light exiting the resonator can be analyzed using a Gaussian-shaped local oscillator beam.

The tolerance requirements for approaching the physical parameters described in Table II are reasonable. For example, for the variant 3 in Table II, the parameters y_0, α, and β have to hold with accuracies about ± 0.25, ± 0.005, and ± 0.005, respectively to keep the value of the loss

TABLE II. Values of the round-trip loss (ppm) for FP cavities having spherical and deformed mirrors, calculated numerically with points number $N = 512$ and window parameter $S = 2$. We used Advanced LIGO parameters summarized in Table I for the FP with spherical mirrors according to a laser spot radius of $w = 0.06$ m on the mirror. AS, D, Q, and M stand for the axial symmetric, dipole, quadrupole, and hexapole modes.

	Modes	AS_{00}	AS_{01}	AS_{02}	D_{10}	D_{11}	Q_{20}	Q_{21}	M_{30}	M_{31}
	Spherical	0.45	170	6500	8.9	1050	100	5100	470	20 000
1	$y_0 = 20$, $\alpha = 0.1525$, $\beta = 0.35$	2.2	46 000	43 000	940	20 000	19 000	30 000	10 000	28 000
2	$y_0 = 27.5$, $\alpha = 0.21$, $\beta = 0$	2.6	46 000	19 000	1100	41 000	23 000	16 000	11 000	30 000
3	$y_0 = 30$, $\alpha = 0.175$, $\beta = -0.05$	3.3	37 000	20 000	1600	36 000	19 000	17 000	8800	12 000

within 3 dB of the predicted values. It means that the shape of the mirrors has to be kept accurate with tolerance $\pm 0.03\lambda$, which is practically feasible. The mirror has to be smooth enough at the wavelength scale for this estimation to be valid.

The considered model of a FP resonator is a simplification of the realistic Advanced LIGO system with one exception. The last one includes two FP resonators and a recycling mirror that allows increasing the effective finesse of the multiresonator system. It is possible to show that the LIGO resonator effective loss is proportional to $T_1T_2/4 + \mathcal{L}_1$, where T_1 and T_2 are power transmission coefficients of the input and recycling mirrors, respectively, and $\mathcal{L}_1$ is the attenuation per round trip in the FP resonator. In the Advanced LIGO interferometer, $T_1 = 0.014$ and $T_2 = 0.03$ [3], so the effective transmission coefficient is about $T_{\text{eff}} = T_1T_2/4 = 100$ ppm, whereas diffraction loss $\mathcal{L}_1 \simeq 0.45$ ppm. The attenuation of the main mode of the resonator has to be small to allow increasing sensitivity of the measurement utilizing nonclassical states of light. Increase of the diffraction loss of this mode by about an order of magnitude (to 5 ppm) seems to be acceptable to use the nonclassical (squeezed) state of light characterized with squeezing parameter $\mathcal{L}_{00}/\mathcal{T}_{\text{eff}} \simeq 0.02$. The increase of the attenuation of the dipole mode beyond 100 ppm results in reduction of parametric instability in accordance with Eq. (1).

Another important factor to consider is related to the dynamic stability of the modified FP cavity. This is discussed in the next section.

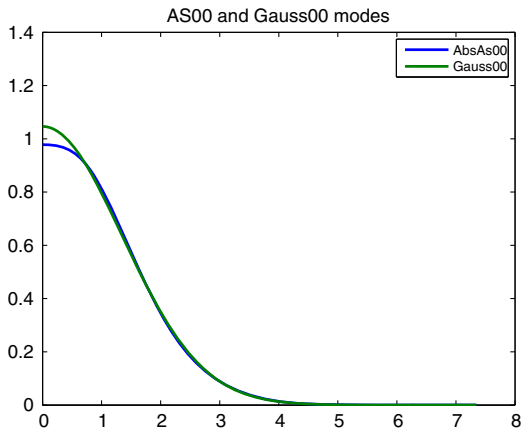

FIG. 4. Amplitude distribution of main AS mode corresponding to parameter set 3 in Table II and the main Gaussian one on the mirror's surface.

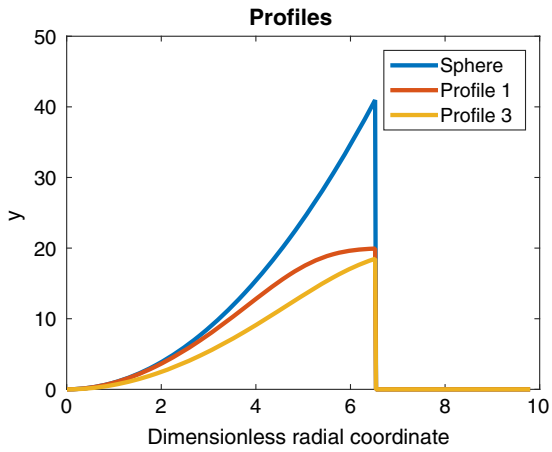

FIG. 5. Mirror shapes (3) for a spherical mirror and mirrors corresponding to sets 1 and 3 in Table II.

IV. TILT STABILITY

The optimization of the mirror's shape results in increase of the diffraction loss of the higher-order FP modes. As a consequence, the diffraction loss of the main mode increases more strongly with the tilt of the mirrors as compared with a conventional FP resonator. The tilt lifts orthogonality and results in linear coupling among the optical modes. The coupling is the largest for the axial symmetric and the dipole modes. It is reasonable to expect that the angle sensitivity of the cavity attenuation is approximately proportional to the square root of the clipping loss value of the dipole mode.

There is no known way of accurate analytical evaluation of the loss increase due to mirror tilt. Moreover, the numerical simulations become rather involved, since the tilt breaks the symmetry of the system. To evaluate this effect, we use a method of successive approximations that is based on a fusion of both the numerical and analytical methods. According to this method, the round-trip loss depends on the small tilt angle θ of one of the mirrors of the FP cavity as

$$\tilde{\mathcal{L}}_{00} \simeq \mathcal{L}_{00}\left\{1+\frac{\theta^2}{\theta^2_{\rm perm}}\right\}, \qquad \frac{1}{\theta^2_{\rm perm}} = \frac{kLS_U}{\mathcal{L}_{00}}, \tag{8}$$

$$S_U \equiv \Re\left[U_{00,00} - 2\sum_j \frac{\Lambda_j^2 |U_{j,00}|^2}{\Lambda_j^2 - \Lambda_{00}^2}\right], \tag{9}$$

$$U_{00,00} \equiv \int |\psi_{00}(x)|^2 x^3 dx, \qquad \int |\psi_j(x)|^2 x dx = 1,$$
$$U_{j,00} \equiv \int \psi_j^*(x)\psi_{00}(x) x^2 dx, \tag{10}$$

where k is the wave number, Λ_j and ψ_j are the calculated numerically forward trip eigenvalue and eigenvector of the unperturbed problem (no tilt), and $\theta_{\rm perm}$ is a permissible angle to characterize the tilt stability.

Numeric calculations for parameter sets 1, 2, and 3 listed in Table II give the following permissible tilt angles:

$$\theta^{(1)}_{\rm perm} \simeq 0.12\ \mu{\rm rad}, \qquad \theta^{(2)}_{\rm perm} \simeq \theta^{(3)}_{\rm perm} \simeq 0.08\ \mu{\rm rad}. \tag{11}$$

To figure out if these values are small enough, we calculate a similar number for the current Advanced LIGO interferometer (Table I) and find $\theta_{\rm LIGO} \simeq 0.6\ \mu$rad. In other words, the dynamic range of the angle deviation of the mirrors of the conventional interferometer is an order of magnitude better than that of the interferometer with the modified mirrors. This is expected, as the loss parameter of the first dipole mode is approximately 1000 ppm (10 ppm) for the single-mode (conventional) resonator.

V. CONCLUSION

In this paper we have shown that it is possible to reduce spectral density in a long-base optical interferometer by properly shaping its mirrors. The mode spectral density reduction is needed to reduce the impact of the parametric instability on the sensitivity of an interferometric gravitational wave detector. The improvement stems from the dependence of the threshold of the instability on the losses of the optical modes involved in the process. Modification of the mirror shape enhances the diffraction loss of the higher-order optical modes, resulting in the instability threshold increase, occurring at the cost of scrutinizing the mirror tilt stability requirements.

To explain and circumvent this effect, we have created a semianalytical model of the diffraction loss of a Fabry-Perot cavity having an arbitrary mirror shape. We have found that optimizing the ratio of the losses of the cavity modes it is possible to achieve a significant suppression of the optomechanic instability and also keep acceptable tolerances of the system implementation. We validated results of our predictions with numerical simulations.

We considered a simplified version of a Fabry-Perot cavity similar to the cavities used in the arms of an Advanced LIGO interferometer. The result of our work is rather suggestive, and deeper theoretical and experimental study is needed to adopt the technique to a full-scaled Advanced LIGO system. The intensity profile of the proposed modes are close to a Gaussian one; however, the changing of the interferometer optics, the impact of the modification of the mirror profile on the optical alignment, and quantum squeezing of the light escaping the dark port require further investigation.

ACKNOWLEDGMENTS

The authors acknowledge fruitful discussions with William Kells. Mikhail V. Poplavskiy and Sergey P. Vyatchanin acknowledge support from the Russian Foundation for Basic Research (Grant No. 14-02-00399A), and the National Science Foundation (Grant No. PHY-130586).

[1] B. P. Abbott *et al.* (LVC Collaboration), Living Rev. Relativity **19**, 1 (2016).
[2] K. Dooley, T. Akutsu, S. Dwyer, and P. Puppo, J. Phys. Conf. Ser. **610**, 012012 (2015).
[3] J. Abadie *et al.*, Classical Quantum Gravity **32**, 074001 (2015).
[4] J. Aasi *et al.* (LIGO Collaboration), Classical Quantum Gravity **32**, 115012 (2015).
[5] B. Abbot *et al.* (LIGO and Virgo Collaborations), Phys. Rev. Lett. **116**, 061102 (2016).
[6] V. B. Braginsky, S. E. Strigin, and S. P. Vyatchanin, Phys. Lett. A **287**, 331 (2001).
[7] M. Arain, V. Quetschke, J. Gleason, L. Williams, M. Rakhmanov, J. Lee, R. Cruz, G. Mueller, D. Tanner, and D. Reitze, Appl. Opt. **46**, 2153 (2007).
[8] J. Sidles and D. Sigg, Phys. Lett. A **354**, 167 (2006).
[9] V. B. Braginsky, S. E. Strigin, and S. P. Vyatchanin, Phys. Lett. A **305**, 111 (2002).
[10] S. E. Strigin and S. P. Vyatchanin, Phys. Lett. A **365**, 10 (2007).
[11] A. G. Gurkovsky and S. P. Vyatchanin, Phys. Lett. A **370**, 177 (2007).
[12] A. Gurkovsky, S. Strigin, and S. Vyatchanin, Phys. Lett. A **362**, 91 (2007).
[13] A. G. Polyakov and S. P. Vyatchanin, Phys. Lett. A **368**, 423 (2007).
[14] M. Evans, L. Bartotti, and P. Fritschel, Phys. Lett. A **374**, 665 (2010).
[15] S. Strigin and S. Vyatchanin, Phys. Lett. A **374**, 1101 (2010).

[16] X. Chen, C. Zhao, S. Danilishin, D. B. L. Ju, H. Wang, S. P. Vyatchanin, C. Molinelli, A. Kuhn, S. Gras, T. Briant *et al.*, Phys. Rev. A **91**, 033832 (2015).
[17] T. J. Kippenberg, H. Rokhsari, T. Carmon, A. Scherer, and K. J. Vahala, Phys. Rev. Lett. **95**, 033901 (2005).
[18] A. B. Matsko, A. A. Savchenkov, V. S. Ilchenko, D. Seidel, and L. Maleki, Phys. Rev. Lett. **103**, 257403 (2009).
[19] A. B. Matsko, A. A. Savchenkov, and L. Maleki, Opt. Express **20**, 16234 (2012).
[20] M. Evans, S. Gras, P. Fritschel *et al.*, Phys. Rev. Lett. **114**, 161102 (2015).
[21] C. Zhao, L. Ju, J. Degallaix, S. Gras, and D. G. Blair, Phys. Rev. Lett. **94**, 121102 (2005).
[22] S. Gras, C. Zhao, D. G. Blair, and L. Ju, Classical Quantum Gravity **27**, 205019 (2010).
[23] J. Degallaix, C. Zhao, L. Ju, and D. G. Blair, J. Opt. Soc. Am. B **24**, 1336 (2007).
[24] C. Zhao, L. Ju, Q. Fang, C. Blair, J. Qin, D. Blair, J. Degallaix, and H. Yamamoto, Phys. Rev. D **91**, 092001 (2015).
[25] S. Gras, P. Fritschel, L. Barsotti, and M. Evans, Phys. Rev. D **92**, 082001 (2015).
[26] S. Gras, D. G. Blair, and C. Zhao, Classical Quantum Gravity **26**, 135012 (2009).
[27] L. Ju, D. G. Blair, C. Zhao, S. Gras, Z. Zhang, P. Barriga, H. Miao, Y. Fan, and L. Merrill, Classical Quantum Gravity **26**, 015002 (2009).
[28] V. B. Braginsky and S. P. Vyatchanin, Phys. Lett. A **293**, 228 (2002).
[29] J. Miller, M. Evans, L. Barsotti, P. Fritschel, M. MacInnis, R. Mittleman, B. Shapiro, J. Soto, and C. Torrie, Phys. Lett. A **375**, 788 (2011).
[30] C. Pare, L. Gagnon, and P. A. Belanger, Phys. Rev. A **46**, 4150 (1992).
[31] M. Kuznetsov, M. Stern, and J. Coppeta, Opt. Express **13**, 171 (2005).
[32] B. Tiffany and J. Leger, Opt. Express **15**, 13463 (2007).
[33] F. Ferdous, A. A. Demchenko, S. P. Vyatchanin, A. B. Matsko, and L. Maleki, Phys. Rev. A **90**, 033826 (2014).
[34] J. Vinet and P. Hello, J. Mod. Opt. **40**, 1981 (1993).